JBC RESEARCH ARTICLE

AMPK phosphorylates PPARδ to mediate its stabilization, inhibit glucose and glutamine uptake and colon tumor growth

Received for publication, April 10, 2021, and in revised form, June 25, 2021 Published, Papers in Press, July 13, 2021,
https://doi.org/10.1016/j.jbc.2021.100954

Jiajun Ding[1,‡], Qian Gou[2,‡], Xiao Jia[1], Qian Liu[3], Jianhua Jin[3], Juanjuan Shi[1,*], and Yongzhong Hou[1,*]

From the [1]School of Life Sciences, [2]School of Medicine, Jiangsu University, Zhenjiang, PR China; [3]Department of Oncology, Affiliated Wujin People's Hospital, Jiangsu University, Changzhou, PR China

Edited by Eric Fearon

Peroxisome proliferator–activated receptor δ (PPARδ) is a nuclear receptor transcription factor that plays an important role in the regulation of metabolism, inflammation, and cancer. In addition, the nutrient-sensing kinase 5′AMP-activated protein kinase (AMPK) is a critical regulator of cellular energy in coordination with PPARδ. However, the molecular mechanism of the AMPK/PPARδ pathway on cancer progression is still unclear. Here, we found that activated AMPK induced PPARδ-S50 phosphorylation in cancer cells, whereas the PPARδ/S50A (nonphosphorylation mimic) mutant reversed this event. Further analysis showed that the PPARδ/S50E (phosphorylation mimic) but not the PPARδ/S50A mutant increased PPARδ protein stability, which led to reduced p62/SQSTM1-mediated degradation of misfolded PPARδ. Furthermore, PPARδ-S50 phosphorylation decreased PPARδ transcription activity and alleviated PPARδ-mediated uptake of glucose and glutamine in cancer cells. Soft agar and xenograft tumor model analysis showed that the PPARδ/S50E mutant but not the PPARδ/S50A mutant inhibited colon cancer cell proliferation and tumor growth, which was associated with inhibition of Glut1 and SLC1A5 transporter protein expression. These findings reveal a new mechanism of AMPK-induced PPARδ-S50 phosphorylation, accumulation of misfolded PPARδ protein, and inhibition of PPARδ transcription activity contributing to the suppression of colon tumor formation.

5′AMP-activated protein kinase (AMPK) is a serine/threonine kinase, which consists of AMPKα (catalytic subunits) and AMPKβ/AMPKγ (regulatory subunits) (1). Activation of AMPK regulates cell growth, metabolism, autophagy, and cancer progression (2, 3). Under intracellular ATP depletion, AMPK is activated and accelerates catabolism, resulting in ATP production. In addition, AMPK can be activated by the upstream regulatory protein LKB1 in the liver (4). Some pharmacologic reagents such as metformin and 5-aminoimidazole-4-carboxamide-1-β-d-ribofuranoside (AICAR) can activate AMPK (2, 5, 6). Activation of AMPK triggers the downstream signaling pathways by inducing the targeted proteins FOXO3a or G-alpha-interacting vesicle-associated protein (GIV) phosphorylation leading to autophagy induction (7) and tumor suppression (8). Furthermore, the interaction of AMPK with peroxisome proliferator–activated receptor δ (PPARδ) regulates glucose metabolism, vascular–endothelial dysfunction, insulin resistance, and inflammation (9–12). AMPK interacts with PPARδ leading to increased endurance or training adaptation in mice (9). Omentin-1 inhibits vascular–endothelial dysfunction in response to high glucose, which is associated with inhibition of the AMPK/PPARδ signaling pathway (10). METRNL alleviates insulin resistance and inflammation in response to lipid or LPS (11, 12), which is involved in activation of AMPK and PPARδ pathways. In addition, PPARδ agonist GW501516-induced glucose uptake of human skeletal muscle cells is AMPK dependent rather than PPARδ (13). As one of the members of PPARs family, PPARδ was the first identified in humans (14), which is highly expressed in colonic epithelial cells and regulates colonic cancer progression (15–20). Ligand-binding and activated PPARδ is involved in the chronic inflammation (ulcerative colitis and Crohn's disease) and colitis-associated colorectal cancer (CRC) (15–19), suggesting that PPARδ activation enhances CRC. Metformin inhibits PPARδ agonist–mediated colorectal tumorigenesis in azoxymethane/dextran sulfate sodium-induced tumor model (21), whereas the molecular mechanism of this pathway on tumor progression is unclear. Here, we identified that AMPK induced PPARδ-S50 phosphorylation leading to inhibition of its transcription activity and PPARδ-mediated tumor growth.

Results

AMPK induces PPARδ phosphorylation

AMPK can be activated by the agonist metformin (22). SW480 cells treated with metformin induced AMPKα phosphorylation and enhanced the interaction of PPARδ with AMPKα by immunoprecipitation analysis (Fig. 1*A*). Confocal analysis showed that AMPKα colocalized with PPARδ (Fig. 1*B*). Further analysis showed that SW480 cells treated with metformin increased PPARδ serine phosphorylation (Fig. 1*C*). AMPK can induce the substrate phosphorylation

‡ These authors contributed equally to this work.
* For correspondence: Yongzhong Hou, houyz@ujs.edu.cn; Juanjuan Shi, sjj@ujs.edu.cn.

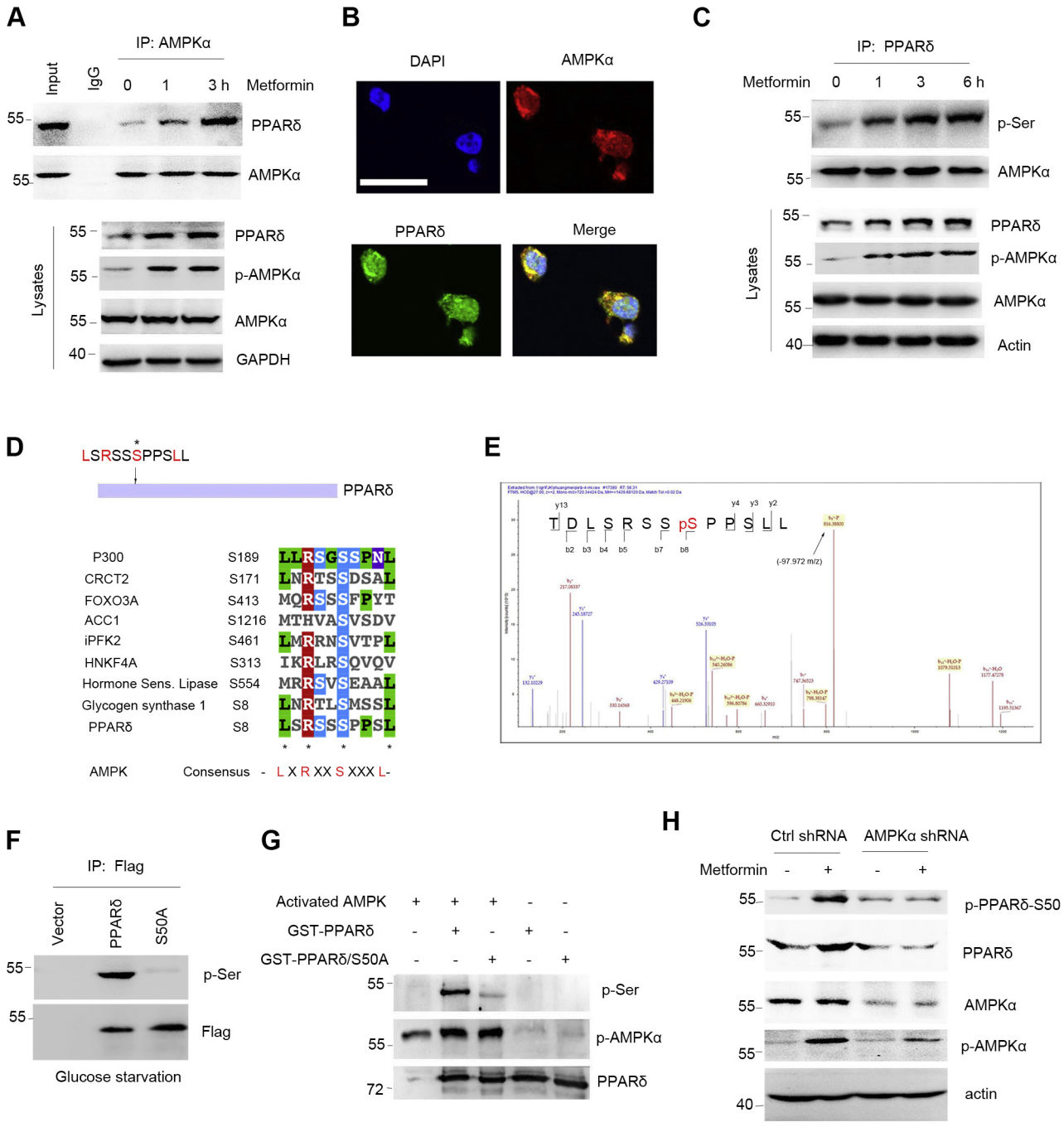

Figure 1. AMPK induces PPARδ phosphorylation. *A*, SW480 cells were treated with metformin (10 mM) as indicated time. Cell lysates were subjected to immunoprecipitation and Western blot. Input: cell lysates from no metformin treatment. *B*, SW480 cells were treated with metformin (10 mM) for 3 h. Cells were subjected to confocal analysis. The scar bar represents 20 μm. *C*, SW480 cells were treated with metformin (10 mM) as indicated time. Cell lysates were subjected to immunoprecipitation and Western blot. *D*, alignment of the consensus of the PPARδ phosphorylation site with AMPK substrates. *E*, SW480 cells were treated with or without glucose starvation for 3 h. Cell lysates were subjected to immunoprecipitation. The purified PPARδ protein was identified by LC/MS/MS. *F*, SW480 cells were transfected with Flag-PPARδ or mutant plasmids for 36 h. After that, cells underwent glucose starvation for 3 h. Cell lysates were subjected to immunoprecipitation and Western blot. *G*, *in vitro* kinase assay was performed as described in Experimental procedures. *H*, SW480 cells were transfected with control shRNA or AMPKα shRNA for 36 h. Cells were treated without or with metformin (10 mM) for 3 h. Cell lysates were subjected to Western blot. AMPK, 5′AMP-activated protein kinase; PPARδ, peroxisome proliferator–activated receptor δ.

with the typical LxRxxSxxxL motif (23); alignment analysis by using https://www.ebi.ac.uk/Tools/msa/clustalo/ shows that PPARδ contains this typical motif (Fig. 1*D*). Glucose starvation can activate AMPK (7). As shown in Figure 1*E*, the 816.388 m/z at b8 ion fragment was from the parent ion neutral loss of one phosphoric acid (97.972 m/z), suggesting that PPARδ-S50 was phosphorylated in response to glucose starvation. To further analyze AMPK-induced PPARδ-S50

phosphorylation, SW480 cells were transfected with PPARδ or PPARδ/S50A mutant and subjected to glucose starvation. As expected, AMPK did not induce PPARδ/S50A mutant phosphorylation (Fig. 1*F*). AMPK-induced PPARδ-S50 phosphorylation was further demonstrated by *in vitro* analysis (Fig. 1*G*). Moreover, AMPKα shRNA-silenced cells inhibited PPARδ-S50 phosphorylation in response to metformin (Fig. 1*H*). These findings suggest that AMPK induced PPARδ-S50 phosphorylation. Interestingly, activated AMPK induced PPARδ-S50 phosphorylation and increased PPARδ protein levels in response to metformin (Fig. 2*A*), AICAR, and glucose starvation (Fig. 2, *B* and *C*). These findings suggest that AMPK induced PPARδ phosphorylation resulting in accumulation of its protein levels.

p62/SQSTM1 induces misfolded PPARδ degradation

Our data showed that AMPK induced PPARδ-S50 phosphorylation, leading to accumulation of PPARδ protein levels, whereas the mechanism is unclear. Further analysis showed that cells treated with the autophagy inhibitor (chloroquine) led to increased PPARδ protein levels (Fig. 3*A*), suggesting that PPARδ undergoes autophagic degradation. Moreover, metformin-treated cells increased PPARδ half-life (Fig. 3*B*). Consistently, the half-life of PPARδ/S50E (mimic phosphorylation) was longer than that of PPARδ/S50A (mimic non-phosphorylation) mutant (Fig. 3, *C* and *D*), suggesting that AMPK induced PPARδ phosphorylation, resulting in inhibition of PPARδ degradation. Western blot analysis showed that AMPK induced the insoluble PPARδ phosphorylation and inhibited its degradation (Fig. 3*E*). p62/SQSTM1 was the first identified autophagy receptor, which can induce the misfolded protein autophagic degradation (24, 25). To address whether p62 could mediate PPARδ autophagic degradation, SW480 cells were transfected with p62 shRNA. Half-life analysis showed that silence of p62 increased PPARδ half-life (Fig. 4*A*). Immunoprecipitation analysis showed that p62 bound to PPARδ (Fig. 4*B*). However, cells treated with metformin inhibited this event (Fig. 4*C*). In addition, compared with PPARδ, PPARδ/S50A mutant significantly enhanced the binding of PPARδ to p62, whereas PPARδ/S50E inhibited this event (Fig. 4*D*). These findings suggest that AMPK induced PPARδ-S50 phosphorylation, leading to inhibition of p62-mediated misfolded PPARδ degradation.

AMPK/PPARδ pathway inhibits cancer cell metabolism

As one of the PPARs family members, PPARδ promotes tumor growth (17, 26–29), which is associated with an increase in tumor metabolism (29). To further address whether PPARδ-S50 phosphorylation could affect its transcription activity, the dual-luciferase analysis showed that S50A mutant significantly increased PPARδ activity compared with the WT (PPARδ) (Fig. 5*A*), and PPARδ agonist GW501516 enhanced this event. However, the S50E mutant reduced PPARδ activity and GW501515 had no effect on PPARδ/S50E activity (Fig. 5*A*). Immunoprecipitation analysis showed that PPARδ/S50A increased the binding of PPARδ to RXRα (a transcriptional partner of PPARδ) (Fig. 5*B*). These findings suggest that PPARδ-S50 phosphorylation disrupted the complex of PPARδ/RXRα, leading to inhibition of PPARδ transcription activity. PPARδ can promote the uptake of glucose and glutamine by increasing the expressions of Glut1 and SLC1A5 (29). As expected, compared with PPARδ, PPARδ/S50E mutant significantly inhibited Glut1 and SLC1A5 gene transcription (Fig. 5, *C* and *D*), which was in agreement with reduced Glut1 and SLC1A5 protein levels (Fig. 5*E*). Consistently, PPARδ/S50E significantly inhibited glucose consumption, lactate release, and glutamine uptake (Fig. 5, *F*–*H*). These findings suggest that PPARδ-S50 phosphorylation inhibited its transcription activity.

AMPK/PPARδ inhibits tumor growth

To further address whether PPARδ-S50 phosphorylation could inhibit cancer cell proliferation and tumor growth, the soft agar analysis and xenograft mouse model were performed. Compared with PPARδ, PPARδ/S50A markedly enhanced cancer cell proliferation and tumor growth, whereas PPARδ/S50E mutant inhibited this event (Fig. 6, *A*–*C*), which was associated with the inhibition of Glut1 and SLC1A5 expressions in S50E-expressed tumors (Fig. 6*D*). These findings suggest that AMPK induced PPARδ-S50 phosphorylation leading to inhibition of PPARδ-mediated tumor growth.

Discussion

PPARs contain PPARα, PPARγ, and PPARδ (30–34). PPARδ can be activated by the fatty acids or fatty-acid derivatives, which is involved in the mucosal inflammation and malignant transformation (26). Aberrant PPARδ expression or activation can cause metastatic progression and carcinogenesis of CRC (15, 16, 26, 29, 35). Consistently, PPARδ KO reduces colon inflammation and colitis-associated tumor growth (17). Conversely, clinical observation shows that higher expression of PPARδ increases survival in patients with CRC (36, 37). Overexpression of PPARδ or activation by agonists decreases CRC cell proliferation and colorectal tumorigenesis (37–40). In contrast, silence or KO of PPARδ promotes colon cancer cell proliferation and tumor growth (41–43). These discrepancy findings could be derived from different models and ligand specificity. AMPK is the metabolic sensor that regulates cellular and organismal metabolism in eukaryotes, which is activated in response to intracellular ATP depletion (2, 22). AMPK plays a critical role in regulating cell growth and metabolism (2). However, the effect of AMPK on PPARδ-mediated cancer cell metabolism and tumor growth is unclear. AMPK induces GIV phosphorylation, leading to stabilization of epithelial tight junctions and inhibition of tumorigenesis (8), suggesting that AMPK can act as a tumor suppressor. Although the AMPK/PPARδ pathway can regulate glucose and lipid metabolism (9, 13, 44–46), the mechanism of this interaction is unclear. Here, we identified that PPARδ contains the typical motif of AMPK phosphorylation substrate (LxRxxS(***50***)xxxL), which was further demonstrated by LC/MS/MS and *in vitro* kinase assay. AMPK induced misfolded PPARδ-S50

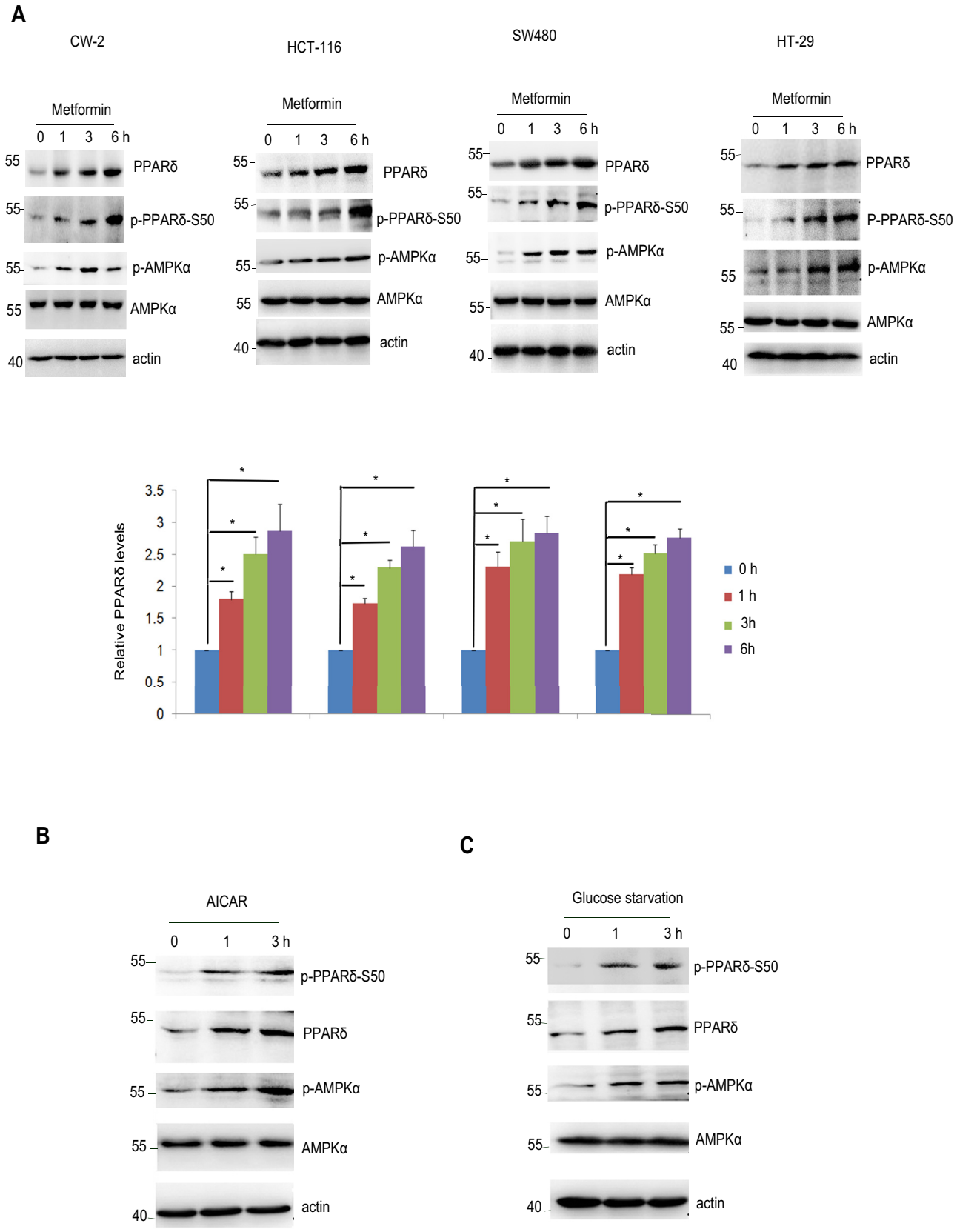

Figure 2. AMPK induces PPARδ-S50 phosphorylation, resulting in accumulation of PPARδ protein levels. *A*, cells were treated with metformin (10 mM) at the indicated time. Cell lysates were subjected to Western blot. The relative PPARδ protein levels were quantified. Results are expressed as the means ± SEM (n = 3). *$p < 0.05$. *B*, SW480 cells were treated with 5 mM AICAR at the indicated time. Cell lysates were subjected to Western blot. *C*, Western blot analysis of SW480 cell lysates in response to glucose starvation. AICAR, 5-aminoimidazole-4-carboxamide-1-β-d-ribofuranoside; AMPK, 5′AMP-activated protein kinase; PPARδ, peroxisome proliferator–activated receptor δ.

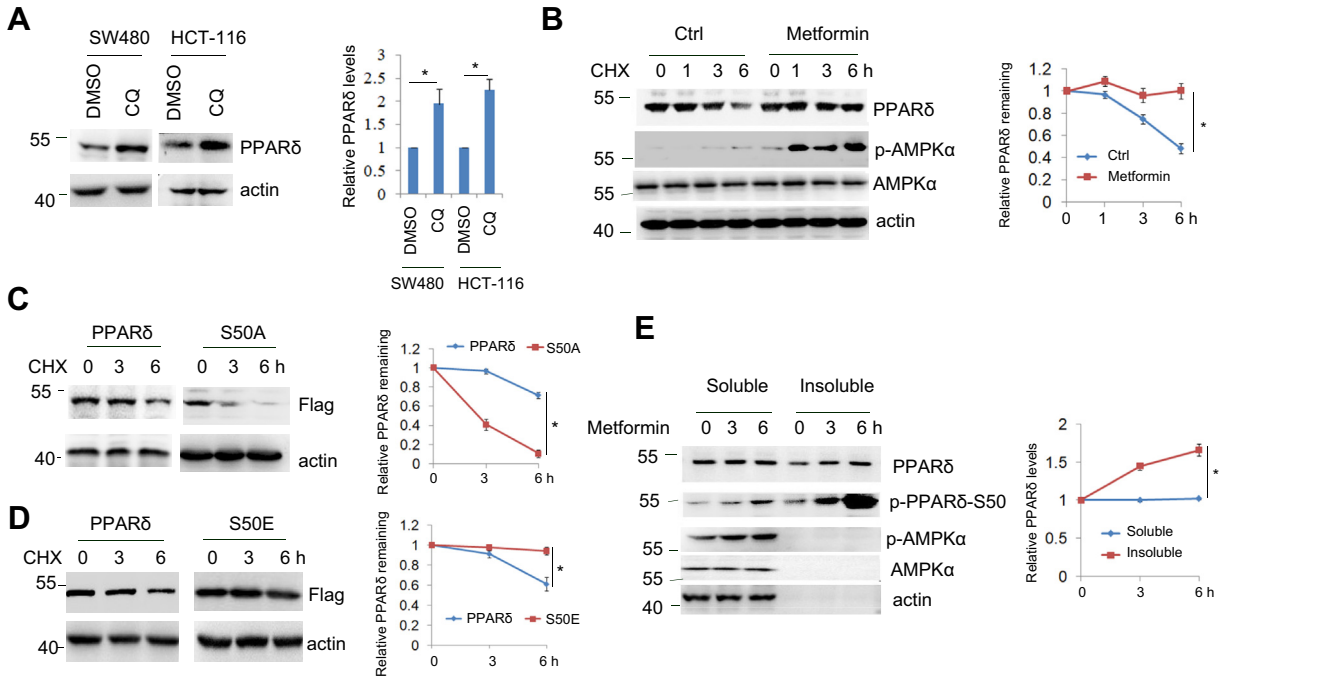

Figure 3. PPARδ-S50 phosphorylation increases PPARδ protein stability. *A*, SW480 or HCT-116 cells were treated with chloroquine (30 μM) for 4 h. Cell lysates were subjected to Western blot. The relative PPARδ protein levels were quantified. Results are expressed as the means ± SEM (n = 3). *$p < 0.05$. *B*, SW480 cells were treated with cycloheximide (30 μg/ml) together with or without metformin (10 mM) at the indicated time. Cell lysates were subjected to Western blot. The relative PPARδ protein remaining at each time point was calculated. Results are expressed as the means ± SEM (n = 3). *$p < 0.01$. *C* and *D*, SW480 cells were transfected with Flag-PPARδ or mutant plasmids for 36 h. Cells were treated with cycloheximide (30 μg/ml) for 0, 3, and 6 h to inhibit *de novo* protein synthesis. Cell lysates were subjected to Western blot. The relative PPARδ protein remaining at each time point was calculated. Results are expressed as the means ± SEM (n = 3). *$p < 0.01$. *E*, SW480 cells were treated with metformin (10 mM) at the indicated time. Soluble and insoluble proteins were extracted as described in Experimental procedures. Extracts were subjected to Western blot. The relative PPARδ protein level at each time point was calculated. Results are expressed as the means ± SEM (n = 3). *$p < 0.01$. PPARδ, peroxisome proliferator–activated receptor δ.

phosphorylation, leading to inhibition of p62-mediated misfolded PPARδ autophagic degradation. Other reports suggest that KRAS could regulate autophagy (47, 48), and SW480 and HCT-116 are KRAS mutant colonic cancer cells, whereas the increased PPARδ protein levels were similar to KRAS WT (CW-2, HT-29) colonic cancer cells (Fig. 2*A*). Protein quality control plays an important role in refolding and degrading misfolded proteins (49–51). Enhanced degradation of misfolded proteins promotes tumorigenesis (52), and cancer cell exhibits the capacity to remove misfolded protein (53). In contrast, the accumulation of misfolded protein is associated with tumor suppression (52, 53). PPARδ-S50 phosphorylation inhibited PPARδ transcription activity, metabolic pathway, and tumor growth, suggesting that AMPK acts as tumor suppressor in cancer cells by inducing PPARδ phosphorylation. Consistently, AMPK induces the downstream GIV phosphorylation leading to tumor suppression (8). Activated PPARδ binds to the peroxisome-proliferator response element (PPRE) consensus sequence (AGGTCANAGGTCA) in the promoter of the target genes and triggers the gene expressions (30–33). Glut1 and SLC1A5 are the direct targets of PPARδ (29), while AMPK induced PPARδ-S50 phosphorylation leading to inhibition of this event, suggesting that PPARδ-S50 phosphorylation suppressed PPARδ-mediated glucose and glutamine metabolic pathways. Glucose metabolism is required for biosynthesis of macromolecules in most types of cancer cells (54). In this process, Glut1 plays a critical role in glucose uptake to maintain cancer cell growth and proliferation (55, 56). In addition, SLC1A5 serves as an important regulator of essential amino acid influx (57). Depletion or silence of SLC1A5 terminates tumor progression (29, 58). Consistent with this, our results showed that AMPK-induced PPARδ-S50 phosphorylation abolished PPARδ transcription activity and reduced uptake of glucose and glutamine and, subsequently, decreased cancer cell proliferation and xenograft tumor growth. Taken together, AMPK induced PPARδ-S50 phosphorylation and reduced PPARδ transcription activity, leading to inhibition of PPARδ-mediated metabolic pathway and tumor growth (Fig. 7).

Experimental procedures

Cells, reagents, and plasmids

The human SW480, HCT-116, HT-29, and CW-2 colonic cancer cell lines were obtained from the ATCC and maintained in 10% fetal bovine serum (FBS, Gibco) Dulbecco's modified Eagle's medium (DMEM). $PPRE_3$-lu plasmid was described previously (31). Human PPARδ cDNA was cloned into the pcDNA3 vector, PPARδ/S50A, or PPARδ/S50E was mutated by the site-directed mutagenesis method and identified by DNA sequencing. The mutant primers: S50A forward: CCCGGAGCTCCGCGCCACCCTCACT; S50A reverse: AGTGAGGGTGGCGCGGAGCTCCGGG. S50E forward: CCCGGAGCTCCGAGCCACCCTCACT; S50E

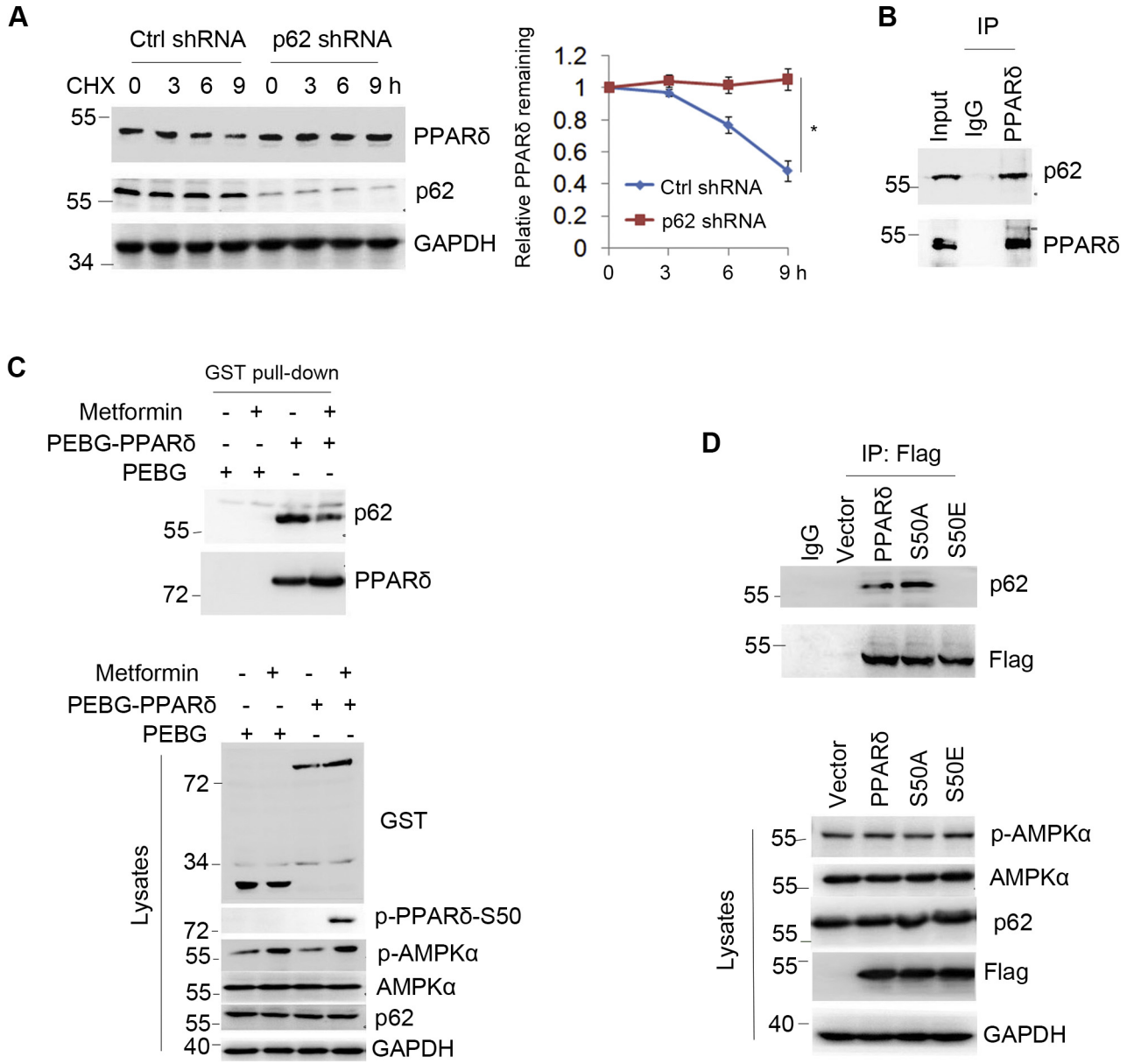

Figure 4. PPARδ-S50 phosphorylation inhibits p62-mediated misfolded PPARδ degradation. *A*, the half-life of PPARδ was assayed in p62 shRNA-silenced SW480 cells. The relative PPARδ protein remaining at each time point was calculated. Results are expressed as the means ± SEM (n = 3). *$p < 0.01$. *B*, cell lysates of SW480 cells were subjected to immunoprecipitation and Western blot. *C*, SW480 cells were transfected with the vector or PEBG-PPARδ for 36 h. Cells were treated with metformin (10 mM) for 1 h as indicated. Cell lysates were subjected to immunoprecipitation and Western blot. *D*, SW480 cells were transfected with Flag-PPARδ or mutant plasmids as indicated for 36 h. Cell lysates were subjected to immunoprecipitation and Western blot. PPARδ, peroxisome proliferator–activated receptor δ.

reverse: AGTGAGGGTGGCTCGGAGCTCCGGG. p62 and AMPKα shRNA plasmids were purchased from GeneChem. Plasmids were transfected into cells by using the TurboFect Transfection Reagent (Thermo Fisher Scientific). AICAR and protease inhibitor cocktail were obtained from Sigma. Metformin was purchased from Bomei biotech. Geneticin (G418 sulfate) was obtained from Thermo Fisher Scientific.

Antibodies and Western blot

PPARδ (Cat: SC-74440) was obtained from Santa Cruz. GAPDH (Cat: 60004) was obtained from Proteintech. p62 (Cat: ab56416) was obtained from Abcam. Actin (Cat: D195316), GST (Cat: D110271), and Flag (Cat: D110005) were purchased from Sangon Biotech. AMPKα (RLT026), phospho-AMPKα1/2 (RLP0575), and anti-phosphoserine (RLM3440) were purchased from Ruiying Biological. The p-PPARδ-S50 mouse polyclonal antibody was developed by using human PPARδ peptide PSSSYTDLSRSS**S**pPPSLLDQL (nonphosphorylation peptide as a negative control), which was purchased from Chinese Peptide Company. Western blot analysis showed that the p-PPARδ-S50 antibody did not cross-react with other PPAR family members (Fig. S1). Secondary antibodies were obtained from Jackson

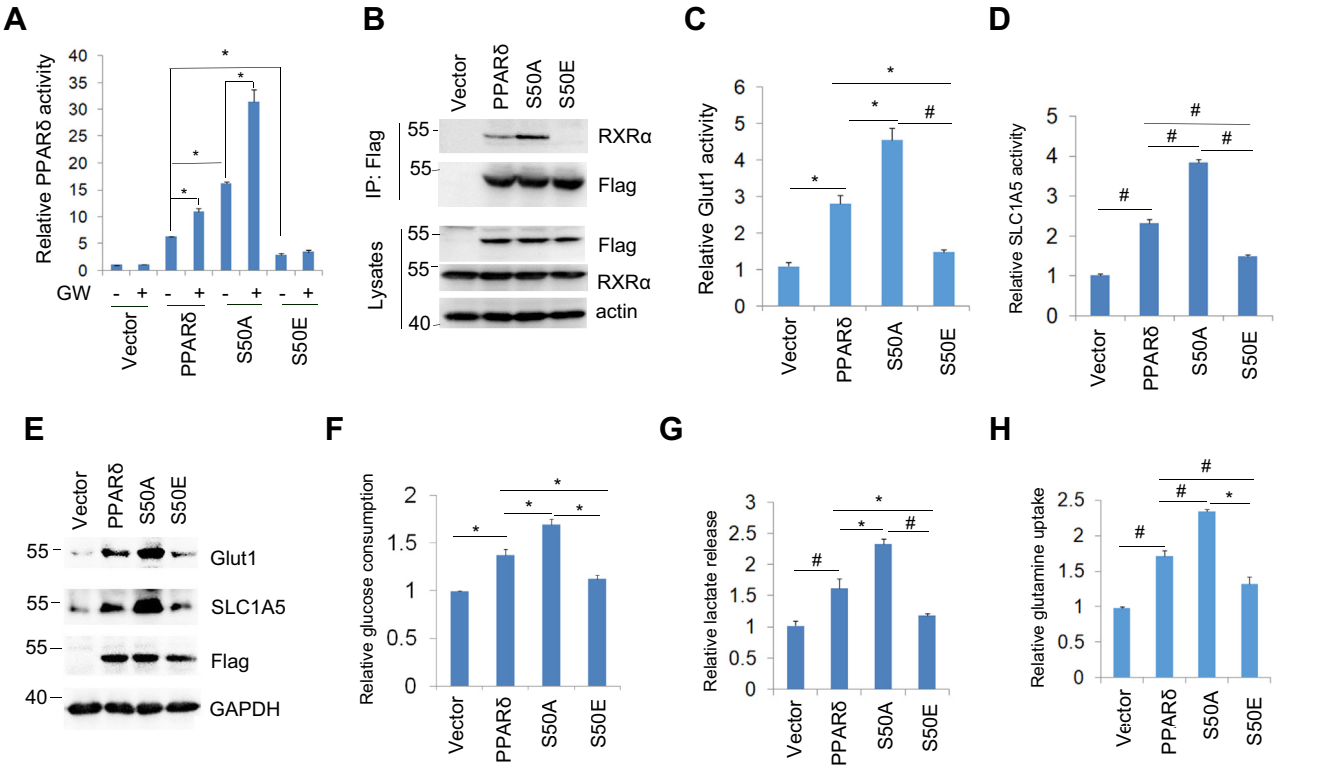

Figure 5. AMPK induces PPARδ phosphorylation leading to inhibition of PPARδ-mediated metabolic pathway. *A*, SW480 cells were transfected with $PPRE_3$-lu reporter plasmids together with PPARδ or mutant plasmids for 36 h. After that, cells were treated with control (DMSO) or GW501516 (10 μM) as indicated for another 12 h. Cell lysates were subjected to dual-luciferase assay. Results are expressed as the means ± SEM (n = 3). $^{*}p < 0.05$. *B*, SW480 cells were transfected with plasmids as indicated for 48 h. Immunoprecipitation and Western blot analysis were performed by using cell lysates. *C* and *D*, SW480 cells were transfected with Glut1-lu or SLC1A5-lu reporter plasmids together with PPARδ or mutant plasmids for 36 h. Cell lysates were subjected to the dual-luciferase assay. Results are expressed as the means ± SEM (n = 3). $^{*}p < 0.05$ and $^{\#}p < 0.01$. *E*, SW480 cells were transfected with PPARδ or mutant plasmids for 36 h. Cell lysates were subjected to Western blot. *F–H*, SW480 cells were transfected with PPARδ or mutant plasmids for 36 h. Relative glucose consumption, lactate release, and L-glutamine uptake were assayed. Results are expressed as the means ± SEM (n = 5). $^{*}p < 0.05$ and $^{\#}p < 0.01$. PPARδ, peroxisome proliferator–activated receptor δ.

ImmunoResearch. Cells were lysed in the lysis buffer (50 mM Tris HCl, pH 7.4, 250 mM NaCl, 0.5% Triton X-100, PMSF, 10% glycerol, protease inhibitor cocktail). Protein concentration was determined by using the Pierce BCA Protein Assay Kit (Thermo). The samples were subjected to SDS-PAGE, transferred to a nitrocellulose membrane, and then probed by the indicated antibodies and developed by using an ECL reagent. Blots were quantified by using ImageJ.

Immunoprecipitation and GST pull-down assay

For immunoprecipitation, cell lysates were precleared with protein A/G PLUS-agarose (Cat: sc-2003, Santa Cruz). Precleared lysates with protein A/G PLUS-agarose beads were added with indicated primary antibodies for 1 h. After that, 15-μl protein A/G PLUS-agarose beads were added and rocked overnight at 4 °C. The beads were washed with ice-cold PBS and subsequently subjected to Western blot with indicated antibodies. For GST pull-down analysis, 15-μl MagBeads GST Fusion Protein Purification (C650031, Sangon Biotech Shanghai) was added to cell lysates and rocked overnight at 4 °C. After that, beads were washed with ice-cold PBS. The samples were subjected to Western blot with the indicated antibodies.

Soluble and insoluble protein fractionation analysis

Cells were incubated with the lysis buffer (50 mM Tris HCl, pH 7.6, 150 mM NaCl, 1% Triton X-100, 30 mM NaF, 1 mM EDTA, protein inhibitors) on ice for 20 min. The lysates were centrifuged at 500*g* for 2 min at 4 °C. The supernatants were further centrifuged at 20,000*g* for 20 min at 4 °C. The supernatants and pellets were collected as detergent-soluble and -insoluble fractions. Insoluble fractions were sonicated. Fractions were subjected to 7% SDS-PAGE and Western blot.

L-glutamine uptake analysis

L-glutamine uptake analysis was described previously (29). After amino acid starvation by FBS deprivation for 20 h, SW480 cells (1×10^4) were incubated with D-PBS buffer (20 mM Hepes and 1 g/l D-glucose, $CaCl_2$, $MgCl_2$) for 3 h. After that, cells were cultured in DMEM containing 4 mM L-glutamine for 45 min. Cells were washed with PBS, and intracellular glutamine levels were measured using the L-Glutamine Assay kit (Goybio) and normalized to total protein levels.

Glucose consumption and lactate release assay

The glucose consumption and lactate release assay were described previously (29). SW480 cells (1×10^4) were grown in DMEM (5.5 mmol/l glucose) with 10% FBS. After cell

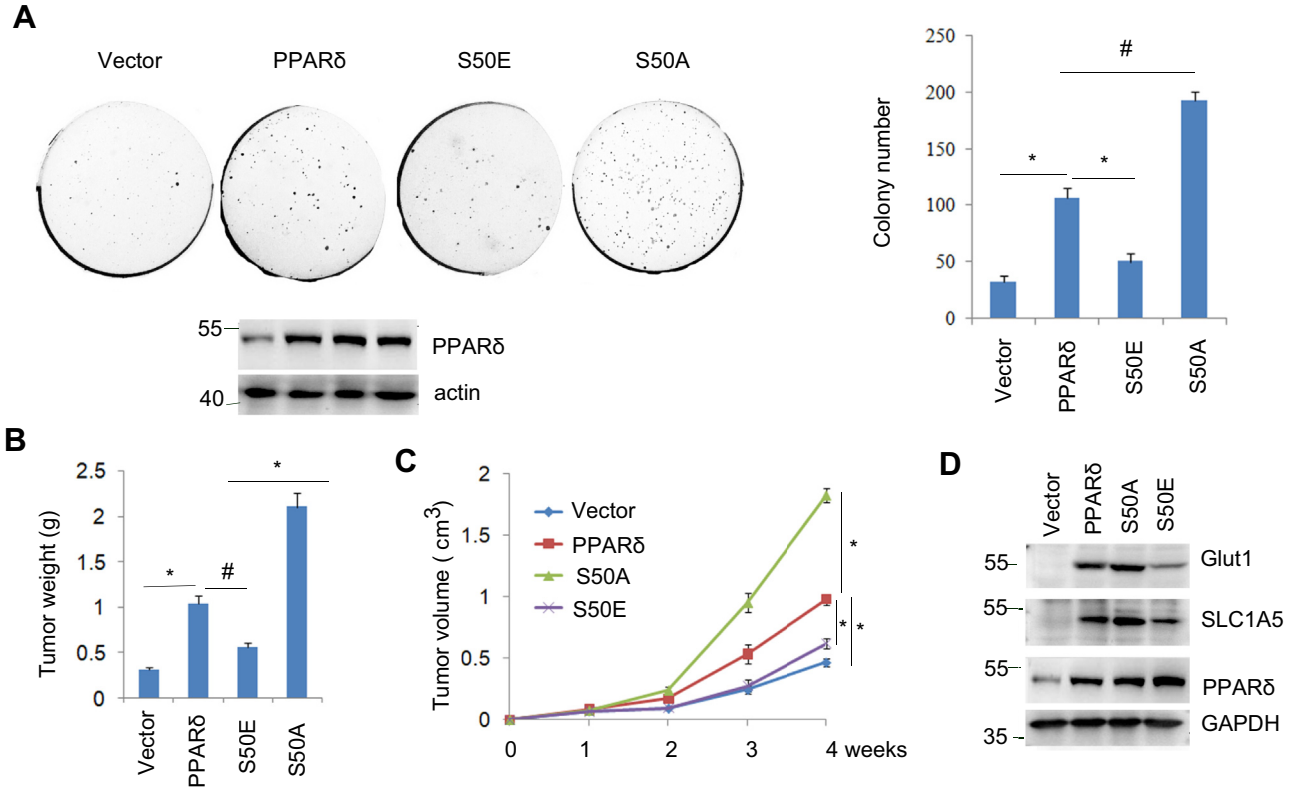

Figure 6. AMPK/PPARδ pathway inhibits tumor growth. *A*, colony formation analysis was performed by using soft agar in stable PPARδ or mutant-expressing SW480 cells. PPARδ or mutant expressions were determined by Western blot. Results are expressed as the means ± SEM, n = 3. *$p < 0.01$ and #$p < 0.05$. *B* and *C*, stable PPARδ or mutant-expressing SW480 cells were injected subcutaneously in nude mice for 4 weeks, and the tumor weight and volume were measured. Results are expressed as the means ± SEM, n = 5. *$p < 0.01$ and #$p < 0.05$. *D*, tumor lysates as indicated were subjected to Western blot. AMPK, 5′AMP-activated protein kinase; PPARδ, peroxisome proliferator–activated receptor δ.

confluence, the medium was discarded, and then, the same FBS/DMEM was added for 12 h. The medium was collected for glucose consumption and lactate release assay. The glucose concentrations were assayed by using the assay kit (Applygen). Lactate release was assayed by colorimetric assay kit (Goybio). The cell number was determined by trypan blue exclusion assay for normalization.

In vitro *kinase assay*

PPARδ cDNA was subcloned into the PGEX-6P-1 vector. The GST-PPARδ or S50A mutant was expressed in *Escherichia coli* strain BL21. The recombinant protein was purified by glutathione-conjugated Sepharose beads. 50 ng purified AMPKα heterotrimers (Signal Chem), GST-PPARδ, or GST-PPARδ-S50A (10 ng) was added in the reaction buffer (20 mM Hepes, pH 7.4, 10 mM $MgCl_2$, 1 mM EGTA, 10 mM ATP, 1 mM DTT) for 40 min at 30 °C. The reactions were subjected to Western blot with indicated antibodies.

MS assay

SW480 cells were treated with or without glucose starvation for 3 h. Cell lysates were subjected to immunoprecipitation by using the PPARδ antibody. Samples with the loading buffer were boiled and then subjected to SDS-PAGE. The gel-purified phosphorylated and unphosphorylated PPARδ proteins were digested with chymotrypsin and trypsin. The digested peptides were assayed by using UPLC-Q-Exactive (Thermo Fisher) at Aixiang Biotech Company in China. Peptide coverage is 78.23% of PPARδ amino acid sequence. The data were searched against UniProt database, and the peptide false discovery rate was <1%.

Immunofluorescent analysis

SW480 cells were treated with metformin (10 mM) for 1 h. Cells were fixed (3.7% paraformaldehyde), permeabilized (0.5% Triton X-100), blocked (10% BSA), and then incubated with the indicated primary antibodies and secondary antibodies (Jackson ImmunoResearch). Immunostained cells were viewed in a confocal microscope.

Luciferase assay

For the PPARδ transcription activity assay, cells were transfected with $PPRE_3$-lu and Ptk-RL together with PPARδ or mutant plasmids for 36 h. Cells were treated with GW501516 as indicated for another 12 h. For the Glut1or SLC1A5 transcription activity analysis, cells were transfected with Glut1-lu or SLC1A5-lu together with Ptk-RL, PPARδ, or mutant plasmids as indicated for 36 h. Cell lysates were assayed by using a dual-luciferase reporter assay system (Promega).

Soft agar analysis

SW480 cells were transfected with PPARδ or mutant (S50A, S50E) plasmids. Cells were selected with G418 to develop

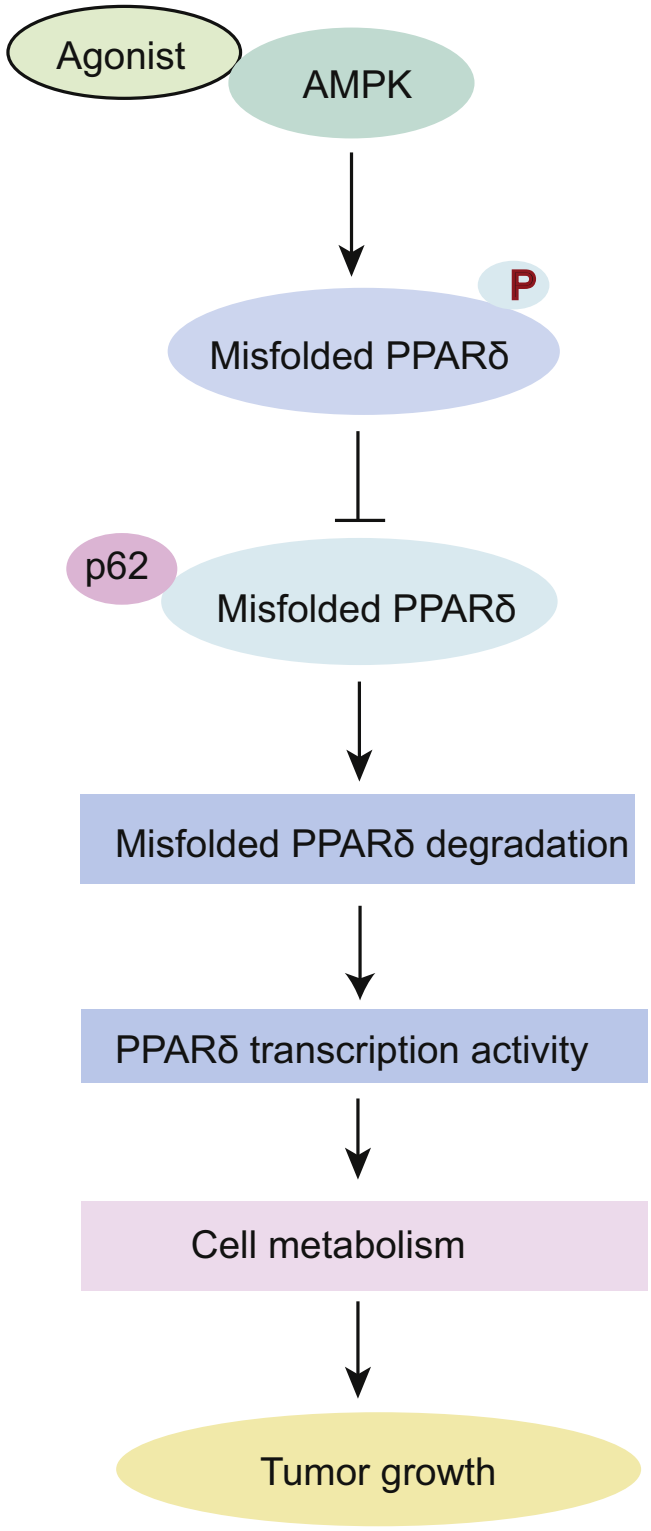

Figure 7. Model of the AMPK/PPARδ pathway inhibits tumor growth. Activated AMPK induced PPARδ-S50 phosphorylation, leading to accumulation of misfolded PPARδ and inhibition of PPARδ transcription activity and subsequently decreased cancer cell metabolism and tumor growth. AMPK, 5′AMP-activated protein kinase; PPARδ, peroxisome proliferator–activated receptor δ.

stable gene-expressing cell lines. Cells (3×10^3) were suspended in 0.35% noble agar with 10% FBS DMEM and were layered over 0.5% agar in six-well plates. A normal culture medium with 500 μg/ml G418 was added to each well. After 2 weeks, dishes were stained with 0.05% crystal violet, and colonies were counted.

Xenograft mouse model

Eight-week-old female NU/NU nude mice were purchased from the laboratory animal center of Yangzhou University. Stable PPARδ, S50A, or S50E expressing SW480 cells (1×10^6) by using G418 selection were injected subcutaneously in nude mice. Each group contains five mice. After 4 weeks, the tumor volume was measured. Tumor volume = 1/2 (length × width^2). All studies were carried out with the approval of the Jiangsu University Animal Care Committee.

Statistical analysis

Data are expressed as the mean ± SEM. Differences between two dependent groups were evaluated with the paired Student's *t* test.

Data availability

Additional data are available as Supplementary information.

Supporting information—This article contains supporting information.

Acknowledgments—This work was supported by the National Natural Science Foundation of China (81972618, 81672711, 81872275), Jiangsu Commission of Health, Natural Science Foundation (M2020002), and Changzhou Sci & Tech Program (Grant No. CJ20200004).

Author contributions—J. D., Q. G., X. J., and Q. L. investigation; J. J. and J. S. methodology; J. J. and J. S. writing–original draft; J. J., J. S., and Y. H. writing–review and editing; J. S. and Y. H. supervision; Y. H. conceptualization; Y. H. project administration.

Conflict of interest—The authors declare that they have no conflicts of interest with the contents of this article.

Abbreviations—The abbreviations used are: AICAR, 5-aminoimidazole-4-carboxamide-1-β-d-ribofuranoside; AMPK, 5′AMP-activated protein kinase; CRC, colorectal cancer; FBS, fetal bovine serum; GIV, G-alpha-interacting vesicle-associated protein; PPARδ, peroxisome proliferator–activated receptor δ; PPRE, peroxisome-proliferator response element.

References

1. Lage, R., Dieguez, C., Vidal-Puig, A., and Lopez, M. (2008) AMPK: A metabolic gauge regulating whole-body energy homeostasis. *Trends Mol. Med.* **14**, 539–549
2. Mihaylova, M. M., and Shaw, R. J. (2011) The AMPK signalling pathway coordinates cell growth, autophagy and metabolism. *Nat. Cell Biol.* **13**, 1016–1023
3. Hardie, D. G. (2015) Molecular pathways: Is AMPK a friend or a foe in cancer? *Clin. Cancer Res.* **21**, 3836–3840
4. Shaw, R. J., Lamia, K. A., Vasquez, D., Koo, S. H., Bardeesy, N., Depinho, R. A., Montminy, M., and Cantley, L. C. (2005) The kinase LKB1 mediates glucose homeostasis in liver and therapeutic effects of metformin. *Science* **310**, 1642–1646

5. Hardie, D. G., Ross, F. A., and Hawley, S. A. (2012) AMPK: A nutrient and energy sensor that maintains energy homeostasis. *Nat. Rev. Mol. Cell Biol.* **13**, 251–262
6. Zhou, G., Myers, R., Li, Y., Chen, Y., Shen, X., Fenyk-Melody, J., Wu, M., Ventre, J., Doebber, T., Fujii, N., Musi, N., Hirshman, M. F., Goodyear, L. J., and Moller, D. E. (2001) Role of AMP-activated protein kinase in mechanism of metformin action. *J. Clin. Invest.* **108**, 1167–1174
7. Shin, H. J., Kim, H., Oh, S., Lee, J. G., Kee, M., Ko, H. J., Kweon, M. N., Won, K. J., and Baek, S. H. (2016) AMPK-SKP2-CARM1 signalling cascade in transcriptional regulation of autophagy. *Nature* **534**, 553–557
8. Aznar, N., Patel, A., Rohena, C. C., Dunkel, Y., Joosen, L. P., Taupin, V., Kufareva, I., Farquhar, M. G., and Ghosh, P. (2016) AMP-activated protein kinase fortifies epithelial tight junctions during energetic stress via its effector GIV/Girdin. *Elife* **5**, e20795
9. Narkar, V. A., Downes, M., Yu, R. T., Embler, E., Wang, Y. X., Banayo, E., Mihaylova, M. M., Nelson, M. C., Zou, Y., Juguilon, H., Kang, H., Shaw, R. J., and Evans, R. M. (2008) AMPK and PPARdelta agonists are exercise mimetics. *Cell* **134**, 405–415
10. Liu, F., Fang, S., Liu, X., Li, J., Wang, X., Cui, J., Chen, T., Li, Z., Yang, F., Tian, J., Li, H., Yin, L., and Yu, B. (2020) Omentin-1 protects against high glucose-induced endothelial dysfunction via the AMPK/PPARdelta signaling pathway. *Biochem. Pharmacol.* **174**, 113830
11. Jung, T. W., Lee, S. H., Kim, H. C., Bang, J. S., Abd El-Aty, A. M., Hacimuftuoglu, A., Shin, Y. K., and Jeong, J. H. (2018) METRNL attenuates lipid-induced inflammation and insulin resistance via AMPK or PPARdelta-dependent pathways in skeletal muscle of mice. *Exp. Mol. Med.* **50**, 1–11
12. Jung, T. W., Pyun, D. H., Kim, T. J., Lee, H. J., Park, E. S., Abd El-Aty, A. M., Hwang, E. J., Shin, Y. K., and Jeong, J. H. (2021) Meteorin-like protein (METRNL)/IL-41 improves LPS-induced inflammatory responses via AMPK or PPARdelta-mediated signaling pathways. *Adv. Med. Sci.* **66**, 155–161
13. Kramer, D. K., Al-Khalili, L., Guigas, B., Leng, Y., Garcia-Roves, P. M., and Krook, A. (2007) Role of AMP kinase and PPARdelta in the regulation of lipid and glucose metabolism in human skeletal muscle. *J. Biol. Chem.* **282**, 19313–19320
14. Schmidt, A., Endo, N., Rutledge, S. J., Vogel, R., Shinar, D., and Rodan, G. A. (1992) Identification of a new member of the steroid hormone receptor superfamily that is activated by a peroxisome proliferator and fatty acids. *Mol. Endocrinol.* **6**, 1634–1641
15. He, T. C., Chan, T. A., Vogelstein, B., and Kinzler, K. W. (1999) PPARdelta is an APC-regulated target of nonsteroidal anti-inflammatory drugs. *Cell* **99**, 335–345
16. Peters, J. M., Morales, J. L., and Gonzalez, F. J. (2011) Modulation of gastrointestinal inflammation and colorectal tumorigenesis by peroxisome proliferator-activated receptor-beta/delta (PPARbeta/delta). *Drug Discov. Today Dis. Mech.* **8**, e85–e93
17. Wang, D., Fu, L., Ning, W., Guo, L., Sun, X., Dey, S. K., Chaturvedi, R., Wilson, K. T., and DuBois, R. N. (2014) Peroxisome proliferator-activated receptor delta promotes colonic inflammation and tumor growth. *Proc. Natl. Acad. Sci. U. S. A.* **111**, 7084–7089
18. Gupta, R. A., Wang, D., Katkuri, S., Wang, H., Dey, S. K., and DuBois, R. N. (2004) Activation of nuclear hormone receptor peroxisome proliferator-activated receptor-delta accelerates intestinal adenoma growth. *Nat. Med.* **10**, 245–247
19. Zhou, D., Jin, J., Liu, Q., Shi, J., and Hou, Y. (2018) PPARdelta agonist enhances colitis-associated colorectal cancer. *Eur. J. Pharmacol.* **842**, 248–254
20. Gou, Q., Jiang, Y., Zhang, R., Xu, Y., Xu, H., Zhang, W., Shi, J., and Hou, Y. (2020) PPARdelta is a regulator of autophagy by its phosphorylation. *Oncogene* **39**, 4844–4853
21. Ding, J., Gou, Q., Jin, J., Shi, J., Liu, Q., and Hou, Y. (2019) Metformin inhibits PPARdelta agonist-mediated tumor growth by reducing Glut1 and SLC1A5 expressions of cancer cells. *Eur. J. Pharmacol.* **857**, 172425
22. Hardie, D. G., Schaffer, B. E., and Brunet, A. (2016) AMPK: An energy-sensing pathway with multiple inputs and outputs. *Trends Cell Biol.* **26**, 190–201
23. Schaffer, B. E., Levin, R. S., Hertz, N. T., Maures, T. J., Schoof, M. L., Hollstein, P. E., Benayoun, B. A., Banko, M. R., Shaw, R. J., Shokat, K. M., and Brunet, A. (2015) Identification of AMPK phosphorylation sites reveals a network of proteins involved in cell invasion and facilitates large-scale substrate prediction. *Cell Metab.* **22**, 907–921
24. Bjorkoy, G., Lamark, T., Brech, A., Outzen, H., Perander, M., Overvatn, A., Stenmark, H., and Johansen, T. (2005) p62/SQSTM1 forms protein aggregates degraded by autophagy and has a protective effect on huntingtin-induced cell death. *J. Cell Biol.* **171**, 603–614
25. Komatsu, M., Waguri, S., Koike, M., Sou, Y. S., Ueno, T., Hara, T., Mizushima, N., Iwata, J., Ezaki, J., Murata, S., Hamazaki, J., Nishito, Y., Iemura, S., Natsume, T., Yanagawa, T., *et al.* (2007) Homeostatic levels of p62 control cytoplasmic inclusion body formation in autophagy-deficient mice. *Cell* **131**, 1149–1163
26. You, M., Yuan, S., Shi, J., and Hou, Y. (2015) PPARdelta signaling regulates colorectal cancer. *Curr. Pharm. Des.* **21**, 2956–2959
27. Jeong, E., Koo, J. E., Yeon, S. H., Kwak, M. K., Hwang, D. H., and Lee, J. Y. (2014) PPARdelta deficiency disrupts hypoxia-mediated tumorigenic potential of colon cancer cells. *Mol. Carcinog.* **53**, 926–937
28. Zuo, X., Peng, Z., Moussalli, M. J., Morris, J. S., Broaddus, R. R., Fischer, S. M., and Shureiqi, I. (2009) Targeted genetic disruption of peroxisome proliferator-activated receptor-delta and colonic tumorigenesis. *J. Natl. Cancer Inst.* **101**, 762–767
29. Jiang, X. M., Xu, Y. L., Huang, M. Y., Zhang, L. L., Su, M. X., Chen, X., and Lu, J. J. (2017) Osimertinib (AZD9291) decreases programmed death ligand-1 in EGFR-mutated non-small cell lung cancer cells. *Acta Pharmacol. Sin.* **38**, 1512–1520
30. Michalik, L., Desvergne, B., and Wahli, W. (2004) Peroxisome-proliferator-activated receptors and cancers: Complex stories. *Nat. Rev. Cancer* **4**, 61–70
31. Hou, Y., Moreau, F., and Chadee, K. (2012) PPARgamma is an E3 ligase that induces the degradation of NFkappaB/p65. *Nat. Commun.* **3**, 1300
32. Hou, Y., Gao, J., Xu, H., Xu, Y., Zhang, Z., Xu, Q., and Zhang, C. (2014) PPARgamma E3 ubiquitin ligase regulates MUC1-C oncoprotein stability. *Oncogene* **33**, 5619–5625
33. Zhang, Z., Xu, Y., Xu, Q., and Hou, Y. (2013) PPARgamma against tumors by different signaling pathways. *Onkologie* **36**, 598–601
34. You, M., Gao, J., Jin, J., and Hou, Y. (2018) PPARalpha enhances cancer cell chemotherapy sensitivity by autophagy induction. *J. Oncol.* **2018**, 6458537
35. Zuo, X., Xu, M., Yu, J., Wu, Y., Moussalli, M. J., Manyam, G. C., Lee, S. I., Liang, S., Gagea, M., Morris, J. S., Broaddus, R. R., and Shureiqi, I. (2014) Potentiation of colon cancer susceptibility in mice by colonic epithelial PPAR-delta/beta overexpression. *J. Natl. Cancer Inst.* **106**, dju052
36. Yang, L., Zhang, H., Zhou, Z. G., Yan, H., Adell, G., and Sun, X. F. (2011) Biological function and prognostic significance of peroxisome proliferator-activated receptor delta in rectal cancer. *Clin. Cancer Res.* **17**, 3760–3770
37. Foreman, J. E., Chang, W. C., Palkar, P. S., Zhu, B., Borland, M. G., Williams, J. L., Kramer, L. R., Clapper, M. L., Gonzalez, F. J., and Peters, J. M. (2011) Functional characterization of peroxisome proliferator-activated receptor-beta/delta expression in colon cancer. *Mol. Carcinog.* **50**, 884–900
38. Hollingshead, H. E., Borland, M. G., Billin, A. N., Willson, T. M., Gonzalez, F. J., and Peters, J. M. (2008) Ligand activation of peroxisome proliferator-activated receptor-beta/delta (PPARbeta/delta) and inhibition of cyclooxygenase 2 (COX2) attenuate colon carcinogenesis through independent signaling mechanisms. *Carcinogenesis* **29**, 169–176
39. Marin, H. E., Peraza, M. A., Billin, A. N., Willson, T. M., Ward, J. M., Kennett, M. J., Gonzalez, F. J., and Peters, J. M. (2006) Ligand activation of peroxisome proliferator-activated receptor beta inhibits colon carcinogenesis. *Cancer Res.* **66**, 4394–4401
40. Zhu, B., Ferry, C. H., Blazanin, N., Bility, M. T., Khozoie, C., Kang, B. H., Glick, A. B., Gonzalez, F. J., and Peters, J. M. (2014) PPARbeta/delta promotes HRAS-induced senescence and tumor suppression by potentiating p-ERK and repressing p-AKT signaling. *Oncogene* **33**, 5348–5359

41. Yang, L., Zhou, Z. G., Zheng, X. L., Wang, L., Yu, Y. Y., Zhou, B., Gu, J., and Li, Y. (2008) RNA interference against peroxisome proliferator-activated receptor delta gene promotes proliferation of human colorectal cancer cells. *Dis. Colon Rectum* **51**, 318–326. discussion 326-318
42. Yang, L., Zhou, J., Ma, Q., Wang, C., Chen, K., Meng, W., Yu, Y., Zhou, Z., and Sun, X. (2013) Knockdown of PPAR delta gene promotes the growth of colon cancer and reduces the sensitivity to bevacizumab in nude mice model. *PLoS One* **8**, e60715
43. Yang, L., Olsson, B., Pfeifer, D., Jonsson, J. I., Zhou, Z. G., Jiang, X., Fredriksson, B. A., Zhang, H., and Sun, X. F. (2010) Knockdown of peroxisome proliferator-activated receptor-beta induces less differentiation and enhances cell-fibronectin adhesion of colon cancer cells. *Oncogene* **29**, 516–526
44. Cheang, W. S., Wong, W. T., Zhao, L., Xu, J., Wang, L., Lau, C. W., Chen, Z. Y., Ma, R. C., Xu, A., Wang, N., Tian, X. Y., and Huang, Y. (2017) PPARdelta is required for exercise to attenuate endoplasmic reticulum stress and endothelial dysfunction in diabetic mice. *Diabetes* **66**, 519–528
45. Bojic, L. A., Telford, D. E., Fullerton, M. D., Ford, R. J., Sutherland, B. G., Edwards, J. Y., Sawyez, C. G., Gros, R., Kemp, B. E., Steinberg, G. R., and Huff, M. W. (2014) PPARdelta activation attenuates hepatic steatosis in Ldlr-/- mice by enhanced fat oxidation, reduced lipogenesis, and improved insulin sensitivity. *J. Lipid Res.* **55**, 1254–1266
46. Choy, K. W., Mustafa, M. R., Lau, Y. S., Liu, J., Murugan, D., Lau, C. W., Wang, L., Zhao, L., and Huang, Y. (2016) Paeonol protects against endoplasmic reticulum stress-induced endothelial dysfunction via AMPK/PPARdelta signaling pathway. *Biochem. Pharmacol.* **116**, 51–62
47. Lo Re, A. E., Fernandez-Barrena, M. G., Almada, L. L., Mills, L. D., Elsawa, S. F., Lund, G., Ropolo, A., Molejon, M. I., Vaccaro, M. I., and Fernandez-Zapico, M. E. (2012) Novel AKT1-GLI3-VMP1 pathway mediates KRAS oncogene-induced autophagy in cancer cells. *J. Biol. Chem.* **287**, 25325–25334
48. Jiffry, J., Thavornwatanayong, T., Rao, D., Fogel, E. J., Saytoo, D., Nahata, R., Guzik, H., Chaudhary, I., Augustine, T., Goel, S., and Maitra, R. (2021) Oncolytic reovirus (pelareorep) induces autophagy in KRAS-mutated colorectal cancer. *Clin. Cancer Res.* **27**, 865–876
49. Balch, W. E., Morimoto, R. I., Dillin, A., and Kelly, J. W. (2008) Adapting proteostasis for disease intervention. *Science* **319**, 916–919
50. Kaur, J., and Debnath, J. (2015) Autophagy at the crossroads of catabolism and anabolism. *Nat. Rev. Mol. Cell Biol.* **16**, 461–472
51. Kim, Y. E., Hipp, M. S., Bracher, A., Hayer-Hartl, M., and Hartl, F. U. (2013) Molecular chaperone functions in protein folding and proteostasis. *Annu. Rev. Biochem.* **82**, 323–355
52. Chen, L., Brewer, M. D., Guo, L., Wang, R., Jiang, P., and Yang, X. (2017) Enhanced degradation of misfolded proteins promotes tumorigenesis. *Cell Rep.* **18**, 3143–3154
53. Tang, Z., Dai, S., He, Y., Doty, R. A., Shultz, L. D., Sampson, S. B., and Dai, C. (2015) MEK guards proteome stability and inhibits tumor-suppressive amyloidogenesis via HSF1. *Cell* **160**, 729–744
54. Boroughs, L. K., and DeBerardinis, R. J. (2015) Metabolic pathways promoting cancer cell survival and growth. *Nat. Cell Biol.* **17**, 351–359
55. Zhao, F. Q., and Keating, A. F. (2007) Functional properties and genomics of glucose transporters. *Curr. Genomics* **8**, 113–128
56. Young, C. D., Lewis, A. S., Rudolph, M. C., Ruehle, M. D., Jackman, M. R., Yun, U. J., Ilkun, O., Pereira, R., Abel, E. D., and Anderson, S. M. (2011) Modulation of glucose transporter 1 (GLUT1) expression levels alters mouse mammary tumor cell growth *in vitro* and *in vivo*. *PLoS One* **6**, e23205
57. Nicklin, P., Bergman, P., Zhang, B., Triantafellow, E., Wang, H., Nyfeler, B., Yang, H., Hild, M., Kung, C., Wilson, C., Myer, V. E., MacKeigan, J. P., Porter, J. A., Wang, Y. K., Cantley, L. C., *et al.* (2009) Bidirectional transport of amino acids regulates mTOR and autophagy. *Cell* **136**, 521–534
58. Jeon, Y. J., Khelifa, S., Ratnikov, B., Scott, D. A., Feng, Y., Parisi, F., Ruller, C., Lau, E., Kim, H., Brill, L. M., Jiang, T., Rimm, D. L., Cardiff, R. D., Mills, G. B., Smith, J. W., *et al.* (2015) Regulation of glutamine carrier proteins by RNF5 determines breast cancer response to ER stress-inducing chemotherapies. *Cancer Cell* **27**, 354–369